Heliyon 9 (2023) e21240

Contents lists available at ScienceDirect

Heliyon

journal homepage: www.cell.com/heliyon

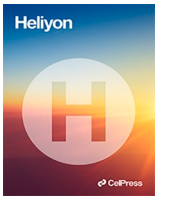

Scintillation and radioluminescence mechanism in β-Ga_2O_3 semiconducting single crystals

A.J. Wojtowicz [a], M.E. Witkowski [a], W. Drozdowski [a,*], M. Makowski [a], Z. Galazka [b]

[a] *Institute of Physics, Faculty of Physics, Astronomy and Informatics, Nicolaus Copernicus University in Toruń, ul. Grudziądzka 5, 87-100, Toruń, Poland*

[b] *Leibniz Institute for Crystal Growth (IKZ), Max-Born-Str. 2, 12489, Berlin, Germany*

ARTICLE INFO

Keywords:
β-Ga_2O_3 single crystals
Semiconducting scintillator
Scintillation and radioluminescence mechanism
Dynamics of charge carrier transport
Trapping
Recombination

ABSTRACT

In this paper, we present the results of experiments on samples of β-Ga_2O_3 single crystals under a project aimed at assessing and improving the scintillation performance of this material by studying scintillation and radioluminescence mechanism and its limitations. In addition to standard experiments, such as scintillation light yields and time profiles, radio-, and thermoluminescence, we developed and tested a new and promising two-beam experiment, in which a sample is excited by an X-ray beam and additionally stimulated by an IR laser diode.

Fe and Mg doping compensate for the inherent n-type conductivity of β-Ga_2O_3 to obtain semi-insulating single crystals for large-area substrates and wafers. At the same time, residual Fe and Ir are ubiquitous uncontrolled impurities leached from the Ir crucibles used to grow large bulk crystals by the Czochralski method.

For these experiments, we selected four samples cut from the Czochralski grown 2-cm diameter β-Ga_2O_3 single crystal boules; one with a reduced Fe content, two unintentionally Fe- and Ir-doped (UID) with lower and higher Fe content, and one doped with Mg.

We find that steady-state radioluminescence spectra measured at temperatures between 10 and 350 K are dominated by the UV emission peaking at about 350–370 nm. Unfortunately, even for the best sample with a reduced Fe-content, the intensity of this emission drops precipitously with the temperature down to about 10 % at 300 K.

From the two-beam experiments, we conclude that recombination via inadvertent Fe impurity involving three charge states (2+, 3+, and 4+) may reduce a steady-state UV emission of β-Ga_2O_3 under X-ray excitation by as much as 60–70 %, one-third to one-half of which is due to the recombination (specific for Fe-doped β-Ga_2O_3) involving the 4+ and 3+ charge states of Fe and the remaining 50–70 % being due to a more familiar route typical of other oxides, involving the 2+ and 3+ charge states of Fe. These losses are at higher temperatures enhanced by a thermally activated redistribution of self-trapped holes (STHs). In addition, the trapping of electrons by Fe and holes by Mg, Fe, and Ir may be responsible for scintillation light loss and reduction of the zero-time amplitude essential for the fast timing scintillation applications.

Despite indirect evidence of competitive recombination in β-Ga_2O_3 involving a deep $Ir^{3+/4+}$ donor level, we could not quantitatively assess losses of the UV steady state radioluminescence light due to the inadvertent Ir impurity.

* Corresponding author.
E-mail addresses: andywojt@fizyka.umk.pl (A.J. Wojtowicz), mwit@fizyka.umk.pl (M.E. Witkowski), wind@fizyka.umk.pl (W. Drozdowski), mimak@umk.pl (M. Makowski), zbigniew.galazka@ikz-berlin.de (Z. Galazka).

https://doi.org/10.1016/j.heliyon.2023.e21240
Received 9 May 2023; Received in revised form 18 October 2023; Accepted 18 October 2023
Available online 26 October 2023

1. Introduction

The wide-bandgap gallium sesquioxide, β-Ga_2O_3, is an emerging and extensively studied material, which has already found numerous applications in electronics and optoelectronics but is also considered for new applications such as gas sensing or detection of ionizing radiations.

The extensive up-to-date review of β-Ga_2O_3 research, including technology, characterization, and applications, was given by Galazka [1], while the first, somewhat overly optimistic report on the scintillation properties of β-Ga_2O_3 was published in 2016 by Yanagida et al. [2]. In particular, Yanagida et al. reported a relatively high scintillation light yield of γ-excited β-Ga_2O_3 at 15,000 ± 1500 photons/MeV. Later a more realistic value was given by Drozdowski et al. [3] (7000 photons/MeV), which they have arranged to confirm at other laboratories [4]. These authors' latest and best figures stand close to 9000 photons/MeV at ambient and about 20,000 photons/MeV at LN_2 temperatures [5]. The earlier systematic light yield and scintillation profile studies of β-Ga_2O_3 have been reported by Mykhaylyk et al. [6] in the temperature range of 7–295 K. Interestingly, while the scintillation light yield (under excitation by α-particles from ^{241}Am) improves upon cooling by a mere 60 %, an astounding peak intensity increase (more than 15 times) is observed in the steady state radioluminescence spectra (X-rays) [6]. Part of this difference may be due to thermally induced scintillation profile changes (traps), but, as pointed out by the authors, the scintillation decay curves are practically unaffected by temperature except below 60 K [6].

Although numerous papers on UV luminescence of β-Ga_2O_3 have been published in the last decade, the essential features of this emission had already been described in two seminal papers [7,8] published some 40–50 years ago. We note that some of the results published by Harwig et al. [8] were obtained on crystals grown by the Verneuil method and some on phosphors (ultra-pure powders). Despite limited experimental capabilities, the authors make a case for a fast ns range decay of the observed UV emission, establish its high quantum efficiency (80 %) at 5 K, and argue for its intrinsic nature. They also suggest that nonradiative intra-center transitions are responsible for low quantum efficiency at higher temperatures and speculate that radiative recombination of self-trapped charge carriers of one sign with the free charge carriers of the other might be responsible for the UV emission.

To substantiate their model, Harwig et al. [8] attempted but failed to measure the EPR spectra of the sample under continuous UV irradiation. Interestingly, a modified experiment of this kind was performed successfully almost 50 years later by Kananen et al. [9], who proved that stable self-trapped holes exist in the X-ray pre-irradiated β-Ga_2O_3 crystals at sufficiently low temperature and for a sufficiently low Fermi level. To lower the Fermi level, the as-grown n-type single crystals were neutron-irradiated to create gallium vacancies (native acceptors).

Kananen et al. [9] proposed a scenario for a lattice relaxation stabilizing a hole on one oxygen ion consistent with the observed hyperfine interactions with Ga nuclei at two equivalent Ga sites. The details agree with a relaxed configuration of the self-trapped hole in β-Ga_2O_3 established by Varley et al. [10] using a DFT approach with a new class of hybrid functionals. These authors also calculated the hole self-trapping energies (E_{ST}) and energy barriers (E_b) for several oxides, including β-Ga_2O_3. They point out that β-Ga_2O_3 displays a unique combination of the highest E_{ST} and the lowest E_b among all the studied materials. They also estimated this material's energy barrier for the hole migration (0.4 eV) along the b-axis. This, in turn, allowed them to evaluate a small polaron hole mobility at 10^{-6} cm^2/Vs. (The measured electron mobility in bulk β-Ga_2O_3 crystals at ambient temperatures is on average 130 cm^2/Vs attaining maximum of 500 cm^2/Vs at 100 K [11]). And finally, based on the agreement between experimental and calculated emission photon energies, Varley et al. concluded that UV luminescence in β-Ga_2O_3 is due to self-trapped holes, as proposed earlier, and presented a schematic configurational coordinate diagram of the relevant UV emission center [10]. The diagram was obtained by calculating total energies for a series of configurations of the system (represented by a supercell of 120 atoms) for interpolated atomic positions between distorted and undistorted minimum energy configurations. However, these calculations have not been extended far enough to allow a theoretical estimate of the energy barrier for intra-center nonradiative transitions.

Interestingly, unlike the energy barrier for nonradiative intra-center transitions, the experimental estimate of the hole-hopping activation energy from the thermal stability of the EPR signals from STHs, V_{Ga}^{2-} (doubly ionized Ga vacancies), and inadvertent Fe^{3+} ions in a sample of β-Ga_2O_3, was possible giving a low value of 190 meV [9]. Unlike V_{Ga}^{2-} and Fe^{3+}, singly ionized Ga vacancies, V_{Ga}^{1-} [12], are observed only before, but not after the initial X-ray irradiation at 77 K when concentrations of V_{Ga}^{1-}, V_{Ga}^{2-}, and Fe^{3+} decrease and those of V_{Ga}^{3-} and Fe^{2+} increase [9]. In this experiment, the EPR signals from STHs, V_{Ga}^{2-}, and Fe^{3+} were measured at 30 K after the sample was warmed to higher consecutive temperatures and annealed for a fixed time. For higher temperatures (between 90 and 110 K), self-trapped holes migrate and recombine with V_{Ga}^{3-} and Fe^{2+}. Consequently, the EPR signal from STHs is reduced for higher temperatures while those of V_{Ga}^{2-} and Fe^{3+} increase [9].

On the other hand, we note that early on, it was observed that Fe ions act as killers of the UV-emission in β-Ga_2O_3 and promote photoconductivity [8,13]. From the data of Harwig et al. [8] the positions of the Fe deep donor levels from which electrons could be transferred to the conduction band, can be roughly estimated at about 0.2 eV above the valence band maximum (VBM).

DFT calculations of Ingebrigtsen et al. [14] for Fe_{Ga}, place such a level at about 0.3–0.5 eV above the VBM. An interesting experimental method based on isothermal recovery curves of the Fe^{3+} EPR signal employed by Gustafson et al. [15], provided a value of 0.70 (±0.05) eV. These curves were measured for two samples; the Mg-doped and Fe-unintentionally doped (UID; 1.4×10^{17} cm^{-3}) crystal, and the Fe-doped crystal (2.5×10^{19} cm^{-3}), at discrete temperatures (250, 255, 260, 265 and 270 K). The positions of the Fe_{Ga} (3+/4+) level calculated from isothermal decays, were almost the same for these two samples. Interestingly isothermal decays of the 325 nm laser light induced Mg_{Ga}^{0} EPR signal at 240, 245, 250, 255, and 260 K in the same Mg-doped sample were measured by Lenyk et al. [16], who, from these measurements estimated the Mg (0/1-) acceptor level position at about 0.65 eV above the valence band maximum (VBM), slightly below the Fe (3+/4+) donor level at 0.7 eV.

Using DLTS, Irmscher et al. established that a major compensating electron trap level in β-Ga_2O_3 was positioned at 0.74 eV below the conduction band minimum (CBM) [12], and eventually, using several experimental techniques and hybrid functional calculations, Ingebrigtsen et al. [15], concluded that the omnipresent trap E2 at ~0.78 eV is due to Fe. They found a strong correlation between the E2 defect and Fe dopant concentrations for several different samples and calculated the energy levels of Fe_{Ga} at 0.61 and 0.59 eV below the CBM for GaII and GaI positions, respectively. These results are reasonably consistent with the previously published and DLTS-measured values. They have also been corroborated by measurements of electrical properties of bulk β-Ga_2O_3 doped with Fe using Ni Schottky diodes which gave activation energies (0.75–0.82) eV and electron capture cross sections (2–5) × 10^{-15} cm^2 [17]. Note that these energies are reasonably consistent with the position of the $Fe^{3+/2+}$ level, measured by Lenyk et al. [18] to be 0.84 (±0.05) eV below the CBM, conduction band minimum. They used the same method (isothermal recovery curves) as Gustafson et al. [15] for the Fe (3+/4+) level and the same, Fe-doped crystal. This result was corroborated by a close resemblance between the measured and simulated thermoluminescence (TL) glow curves (measured with the heating rate, β = 1 K/s) in which the $Fe^{3+/2+}$ level played a role of the TL electron trap [18]). Lenyk et al. found, using filters, that most of the TL light emitted in this experiment was contained between 500 and 600 nm [18].

In summary, we note that Fe_{Ga} in β-Ga_2O_3 can act as a deep acceptor introducing a (3+/2+) level below the CBM, and, alternatively, as a deep donor introducing a (3+/4+) level above the VBM. This unique feature of Fe_{Ga} in β-Ga_2O_3 can be explained by a relatively large band gap of β-Ga_2O_3. In smaller bandgap Ga-compounds, like e.g. GaAs (1.42 eV), and GaN (3.4 eV), only a 3+/2+ level has been identified at about 0.96 eV (GaAs) and 1.54 eV (GaN) below the CBM (see Refs. [19,20], respectively). The presence of two Fe levels in the forbidden energy gap of β-Ga_2O_3 is likely to promote two different modes of e-h recombination via Fe_{Ga} in β-Ga_2O_3:

$$\text{mode I}: e_c + h_v + Fe_{Ga}^{3+} \rightarrow Fe_{Ga}^{2+} + h_v \rightarrow Fe_{Ga}^{*3+} \rightarrow Fe_{Ga}^{3+} + h\nu_{IR}$$

and

$$\text{mode II}: e_c + h_v + Fe_{Ga}^{3+} \rightarrow Fe_{Ga}^{4+} + e_c \rightarrow Fe_{Ga}^{*3+} \rightarrow Fe_{Ga}^{3+} + h\nu_{IR}$$

in which three different, quasi-stable charge states, 2+, 3+, and 4+, of the Fe ion play a role. e_c, h_v, Fe_{Ga}^{*3+}, and $h\nu_{IR}$ stand for an electron in the conduction band, a hole in the valence band, the excited Fe_{Ga}^{3+} ion and an infrared photon. The infrared emission in Fe-doped GaN is due to mode I and has been identified as due to the $^4T_1(G) \rightarrow {}^6A_1(S)$ transition of the Fe^{3+} ion. This emission consists of the vibrational sideband and the ZPL (zero-phonon line) peaking at about 1.299 eV [20]. In β-Ga_2O_3, for both modes, whichever is active, one UV photon will be replaced by one Fe^{3+} infrared photon, effectively lowering the quantum efficiency of the UV emission. This is the mechanism of "non-radiative" quenching of the UV emission in β-Ga_2O_3 by a "luminescence killer", the Fe^{3+} ion.

The last potentially significant and unintentionally introduced impurity in β-Ga_2O_3 is Ir, detected, studied, and reported in 2018 by Ritter et al. [21] in Mg-doped samples of β-Ga_2O_3. A preponderance of Ir^{4+} in such samples (Ir donors compensated by Mg acceptors), was also confirmed by a resonant electronic Raman scattering from Ir^{4+} ions reported by Seyidov et al. [22]. The transmission spectrum and the configuration coordinate diagram point to the $Ir^{4+/3+}$ charge transfer transition (from the valence band to the empty Ir^{3+} ground state level) with a zero-phonon line at about 2.6 eV, which would suggest the 2.25 eV threshold for the optically induced increase of the Ir^{4+} and decrease of the Fe^{3+} steady state photo-EPR signal at 30 K (2.25 + 2.6 = 4.85 eV) [21]. Interestingly, in a pre-irradiated Fe-doped β-Ga_2O_3 crystal (using the above-band-gap photons), in addition to the 2.2 eV threshold, there is also a threshold at 1.2 eV. At this threshold, the Fe^{3+} EPR signal starts to increase, while the Ir^{4+} EPR signal starts to decrease [23,24]. This demonstrates that 1) it is possible to convert Fe^{2+} into Fe^{3+} by irradiating the sample with the 1.2 eV light and moving electrons to the conduction band, and 2) Ir^{4+} ions can capture electrons from the conduction band and change their charge state to 3+, as expected. As Lenyk et al. [18] show, the $Ir^{4+} + e_{cb} \rightarrow Ir^{3+}$ recombination process has a measurable, longer wavelength radiative component (between 500 and 600 nm) detected as a TL signal. To prove that Ir^{3+} can work as a recombination center for free electron-hole pairs, it remains to demonstrate that it can also capture a hole from the valence band. This has been shown by Lenyk et al. [25] for the Fe-doped β-Ga_2O_3 sample using ionizing radiation (X-rays). They observe a decrease in Fe^{3+} and an increase in Ir^{4+} EPR signals upon X-ray irradiation. Remarkably, however, for a different, Mg-doped β-Ga_2O_3 sample, both Fe^{3+} and Ir^{4+} EPR signals decrease. This time, Ir^{4+} ions compete with Fe^{3+} ions for electrons from the conduction band since most of the holes from the valence band are captured by the Mg acceptors, not Ir^{3+}. In conclusion, deep Ir^{3+} donors can recombine free electrons and holes in β-Ga_2O_3 via the process involving its 4+ and 3+ charge states.

2. Samples and experimental set-up

All the experiments reported in this paper were performed on four samples of the bulk β-Ga_2O_3 single crystals showing a varying degree of Fe contamination as inferred from the X–IR experiment; one with a reduced Fe content (labeled A), two unintentionally Fe- and Ir-doped (UID) with lower (labeled B) and higher (labeled C) Fe and Ir content, respectively, and one Mg-doped (labeled D), showing the highest unintentional Fe contamination. The crystals were grown at Leibniz-Institut für Kristallzüchtung, Berlin, Germany. Research and development of technology of β-Ga_2O_3 have been documented in detail in several papers (see Galazka et al. [1] and references therein). The electrical and scintillation properties of four samples, listed in Table 1, have been measured and reported before (see Refs. [3,5,11], respectively).

Steady-state radioluminescence (RL) spectra and low temperature thermoluminescence (ltTL) glow curves were measured using a typical set-up, shown in Fig. 1. The set-up consists of the Inel XRG3500 X-ray generator (45 kV/10 mA), the ARC SP 500i monochromator set to the 0th order, the Hamamatsu R928 PMT, and the APD Cryogenics closed-cycle helium cooler controlled by the Lake

Shore 330 Temperature Controller unit.

Usually, the sample was irradiated by X-rays for 10 min at 10 K before the TL runs, in which a typical heating rate was 0.145 K/s. The Thorlabs 830 nm, 1 W IR pulsed laser diode was added to the set-up so that both X-ray and IR-laser beams were directed at the sample in the He-cooler. Both beams could be turned on and off as desired. From seven timing sequences proposed by Poolton et al. [26], and designed for studies of charge competition, trapping and luminescence efficiency in wide band-gap materials, we have chosen three particular sequences (I, II, IV as defined in Ref. [26]), which we labeled s1, s2, and s4 (note that the s1 sequence is equivalent to the typical Optically Stimulated Luminescence, OSL experiment). The IR-laser beam was also used as an additional stimulation in the ltTL experiment that followed the X-ray irradiation.

3. Results and discussion

3.1. Steady state radioluminescence

In Fig. 2 we present steady-state radioluminescence spectra of four β-Ga_2O_3 single crystals, labeled A, B, C, and D, measured at 10 K. The spectra show two well-known bands, a UV-emission band (peaking at 350–370 nm; 3.54–3.35 eV) and a second, red-shifted emission band labeled UV' (peaking at about 400 nm; 3.10 eV), see e.g. Ref. [27].

As reported earlier, Al-doping is responsible for some blue shifts as the UV band peak positions for Al-doped samples in Fig. 2 and published in the literature are at somewhat shorter wavelengths suggesting the shift and, therefore, the increase of the energy gap. Interestingly, while the maximum peak shift in emission spectra (for the highest doping concentration of Al at 5 mol.%) is about 0.19 eV, the bandgap increase from the absorption edge shift is only about 0.11 eV [28].

In Fig. 3, we present steady-state radioluminescence spectra of the β-Ga_2O_3:Al, Ce single crystal, labeled A, measured at several temperatures from 10 to 350 K. The key observation in this experiment is the strong quenching of both emission bands, UV and UV', with temperature. The peak intensity of the UV-band at 300 K is only about 10 % of the 10 K value.

Interestingly, for powder phosphors, the thermal quenching of the UV emission is even stronger as the 200 K peak intensity value is only about 6 % of the 5 K value [8]. This clearly shows that, not unexpectedly, there must be a high external quenching of the UV-emission in powders, but it remains to be determined whether or not there is also a significant intra-center quenching in both powders and single crystals of β-Ga_2O_3.

To get some idea about intra-center nonradiative transitions in the strongly lattice-coupled luminescence center, one may resort to the simplest version of the configurational coordinate model of such a center (one configurational coordinate and a linear approximation for the distortion energy term in the relaxed, adjusted configuration of ions in the excited state). In the case of UV-emission in β-Ga_2O_3, the center would consist of the self-trapped hole STH (located at the O^{1-} ion) and a loosely bound electron e_{cb}* [8,10]. Three parameters, the bandgap energy E_g (4.85 eV) and two UV-emission band parameters, namely the peak energy (3.41 eV) and the estimated position of the zero-phonon line (4.13 eV) suffice to construct such a diagram as shown in Fig. 4.

From the diagram, we obtain two energies, $E_b \sim 0$, $E_{ST} \approx 0.72$ eV, which can be compared to the values calculated by Varley et al. [10] using a modified DFT approach ($E_b \approx 0.1$ eV, $E_{ST} \approx 0.53$ eV).

To summarize, the most important conclusions from this diagram are that free holes in β-Ga_2O_3 crystals self-trap almost immediately and that the energy barrier for the intra-center nonradiative transitions is so high that they cannot contribute to the thermal quenching of the UV emission between 10 and 300 K. Strictly speaking the UV emission is not "thermally quenched"; it is, most likely, the effective concentration of the excited UV centers formed under the constant, steady state excitation, which strongly decreases with temperature as the activation energy for hopping of holes between oxygen ions is only 0.19 eV, much less than 0.72 eV, as expected [10].

The temperature dependence of the total wavelength integrated emission intensities for all four samples is shown in Fig. 5. It is interesting to note that only one sample, A, does not show a drop in intensity at temperatures between 80 and 120 K. At these temperatures, as shown by Kananen et al. [9], the self-trapped holes become unstable, migrate to and, in their experiment, recombine with triply charged gallium vacancies V_{Ga}^{3-} and Fe^{2+} ions. Since in our crystals, unlike crystals studied by Kananen et al. [9,12], no significant concentration of gallium vacancies is expected, the most likely scenario in our experiment is the recombination of mobile self-trapped holes with inadvertent Fe^{2+} ions. This would explain the observed drop in intensity for samples B, C, and D between 80 and 120 K.

Table 1
Samples of β-Ga_2O_3 used in this study.

Label	dopant concentrations (mol. %) [a]	analyte (Fe, Ir, Mg, Zr) concentrations in crystals (cm^{-3}) [b]	free carrier concentration (cm^{-3}) [11]	scint. Light yield (ph/MeV) [3,5]
A	5 (Al), 0.25 (Ce)	3.2×10^{17} (Mg)	8.0×10^{15}	3500 ± 200
B	5 (Al)	< LOQ	insulator	1300 ± 100
C	2.5 (Ce)	6.6×10^{16} (Ir)	insulator	300 ± 50
D	0.2 (Mg)	2.1×10^{18} (Mg); 1.0×10^{16} (Zr)	insulator	300 ± 50

[a] Dopant concentrations relate to concentrations in the melt.

[b] Analyte concentrations measured and evaluated by ICP-OES at *Leibniz-Institut für Kristallzüchtung*. Fe, Ir, Mg and Zr concentrations are given in cm^{-3} if in excess of LOQ (a limit of quantification) at 1.8×10^{17}(Fe), 1.5×10^{16}(Ir), 2.4×10^{17}(Mg) and 2.0×10^{15}(Zr). None of the samples contains inadvertent Fe in excess of LOQ.

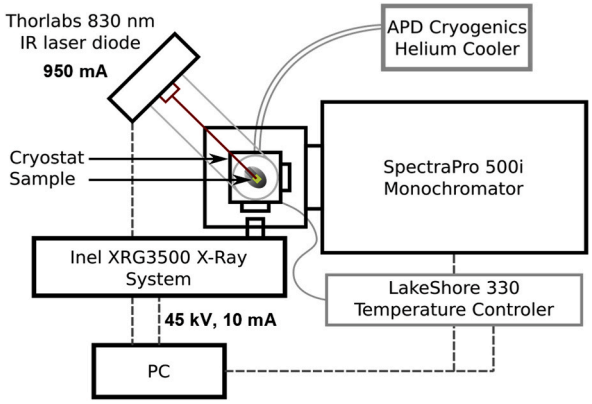

Fig. 1. Experimental set-up.

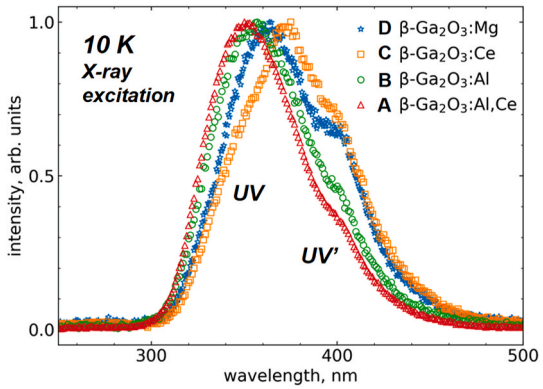

Fig. 2. Steady-state radioluminescence spectra of β-Ga_2O_3 single crystals, labeled A, B, C, and D (see Table 1) measured at 10 K. X-ray beam parameters were 45 kV/10 mA, the IR laser beam was turned off. The spectra have not been corrected for the spectral sensitivity of the set-up.

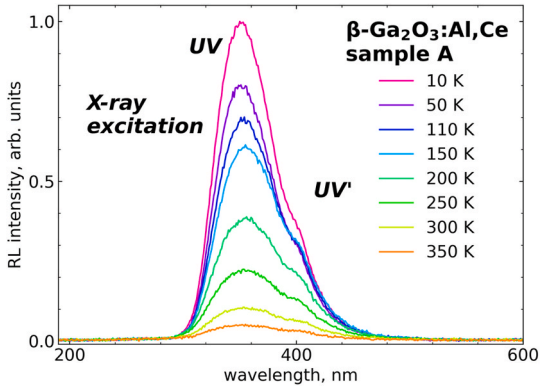

Fig. 3. Steady-state radio-luminescence spectra of the β-Ga_2O_3: Al, Ce single crystal (labeled A) at different temperatures, as indicated in the figure. X-ray beam parameters were 45 kV/10 mA; the IR laser beam was turned off. The spectra have not been corrected for the spectral sensitivity of the set-up.

Then, the conclusion is that the concentration of unintentional Fe ions in sample A must be much lower. Also, note that the scintillation efficiency of this sample is the highest of all the samples listed in Table 1.

3.2. Thermoluminescence

In Fig. 6, we present two different thermoluminescence measurements for all four samples listed in Table 1; a standard ltTL (low temperature thermoluminescence measured after 10 min, X-ray irradiation at 10 K; shown by broken blue lines) and IR-stimulated low

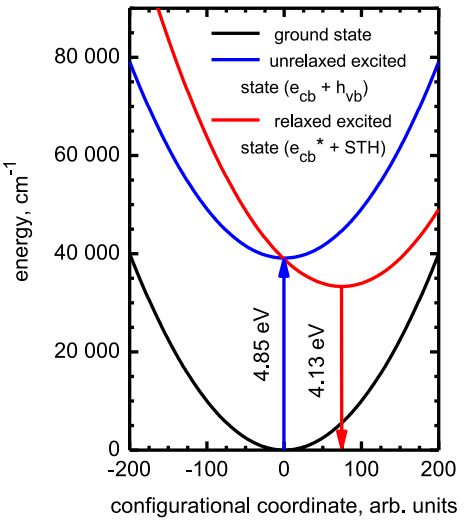

Fig. 4. Configurational coordinate diagram of the UV-center in β-Ga_2O_3 showing a) total energy of the system for the ground state (no e-h pair; the selected O^{2-}; black line), b) the excited unrelaxed state (free e-h pair, the selected O^{2-} ion and the same configuration of the ions surrounding it; blue line), and c) the excited relaxed state (a loosely bound electron and a hole localized at the O^{-} ion; the configuration of the ions adjusted to minimize the potential energy of the system; red line).

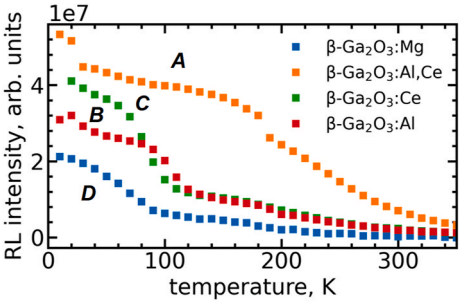

Fig. 5. The wavelength integrated total steady-state radioluminescence intensities of the A, B, C, and D samples of β-Ga_2O_3 from Table 1, as a function of temperature.

temperature thermoluminescence, shown by broken red lines. In the latter case, standard X-ray irradiation was followed by a 1 s pulse from the IR laser before the glow curves were measured.

Sample A (Fig. 6a, β-Ga_2O_3: Al, Ce) shows four TL glow peaks at 35, 115, 205, and 300 K ("no-IR" blue line). The 35 K peak is generated by traps at 0.023 eV below CBM, due to the shallow effective-mass donors [11]. For detailed account of TL experiments and interpretations see Ref. [29]), Electrons released from these traps to the conduction band recombine radiatively with STHs (self--trapped holes), generating UV emission [29]. The Fermi level at equilibrium (before X-ray irradiation) must be high since this sample shows some conductivity at ambient temperatures. It can't be and isn't too high, as part of the shallow donor traps must be empty before X-ray irradiation. This circumstance typically occurs because of partial compensation, in this case, almost certainly, by inadvertent Mg ions (see Table.1). Note that at temperatures covered by this glow peak, the STHs are stable [9] and can serve as recombination partners for the excess electrons released thermally from the shallow donor traps to the conduction band.

The next glow peak, at 115 K, although very weak for sample A, displays a much higher intensity for sample B. Then, for sample C, it becomes very weak again. We have already suggested that this peak might be due to recombination involving thermally "untrapped" mobile STHs (hole traps) and unintentional Fe^{2+} ions (recombination centers).

If this suggestion were valid, one would expect a radiative component of this recombination to correspond to the mode I recombination of free electrons and holes via Fe_{Ga}. This mode of recombination was shown, for GaN, to lead to the Fe^{3+} $^4T_1 \rightarrow {}^6A_1$ emission with a zero-phonon line at 954 nm (1.299 eV) [20,30], which is not expected to shift very much in β-Ga_2O_3. We note, however, that the R928 PMT we use would be insensitive at this wavelength range. Interestingly, Sun et al. [31] proposed that in Fe-doped β-Ga_2O_3, energy transfer from the higher levels of the excited Fe^{3+} ions to the inadvertent Cr^{3+} ions leads to the easily detectable characteristic red Cr emission despite the low Cr concentration. The effect would be even more substantial for a higher concentration of Fe, and the thermoluminescence intensity in the 115 K peak, as seen by the IR-insensitive PMT, would be even higher. So, it seems that we can detect and record the 115 K peak only because the excited Fe^{3+} ions do not always relax to their $^4T_1$ emitting level but transfer their

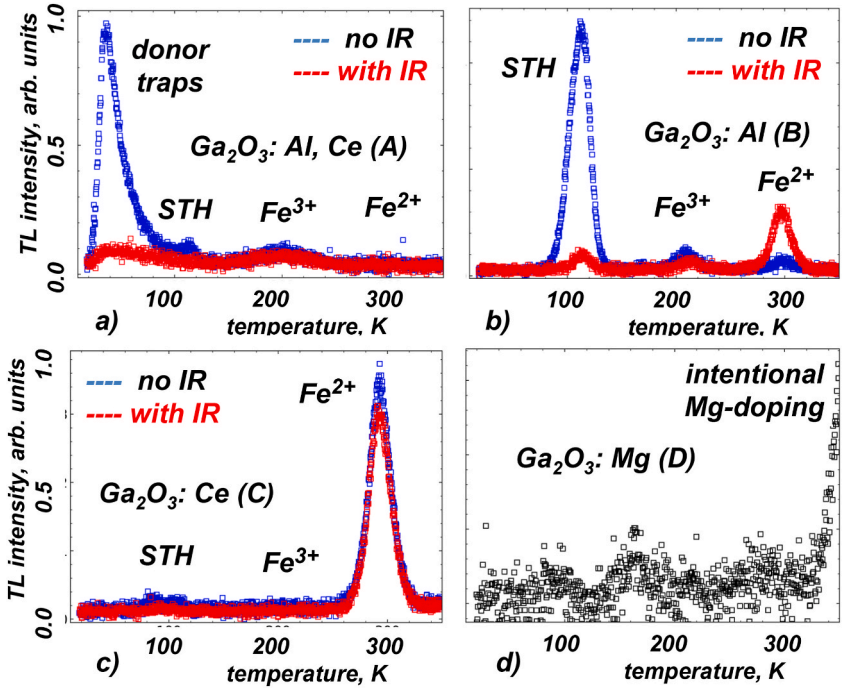

Fig. 6. The wavelength unresolved ltTL (low temperature thermoluminescence) glow curves of samples from Table 1: a) β-Ga_2O_3: Al, Ce (A), b) β-Ga_2O_3: Al (B), c) β-Ga_2O_3: Ce (C), d) β-Ga_2O_3: Mg (D). The glow peak labels indicate the charge states of the subset of Fe ions responsible for a given peak (a trap assigned to a given glow peak) after the X-ray irradiation.

energy to Cr^{3+} ions. More experimental studies are needed to support this somewhat unusual conjecture.

The origin of the 205 K peak is not entirely clear either; we tentatively assign it to the Fe^{3+} hole trap level (upon hole trapping, the ion assumes a 4+ charge state), although we note that the isothermal decays of Fe^{4+} ions measured by Gustafson et al. by a proxy of the Fe^{3+} EPR signal [15], occurred at higher temperatures around 250 K. Ignoring this difference for now, we would assume a scenario in which after holes are released from Fe^{4+} ions to the valence band, they recombine with electrons trapped at Fe^{2+} ions. Similarly, the origin of the 300 K glow peak, clearly visible in sample B, can be assigned to the Fe^{2+} deep acceptor electron trap level from which an electron would be thermally released at about 300 K. This was directly demonstrated by Lenyk et al. [18], who measured isothermal recovery curves of the Fe^{3+} EPR signal at several temperatures around 300 K. They also used long pass filters to identify a spectral range covered by thermoluminescence released at these temperatures and concluded that most of it had wavelengths between 500 and 600 nm and, most likely, was due to the radiative recombination of electrons released from the Fe^{2+} ions with Ir^{4+} ions (valence band holes trapped at Ir^{3+} ions). Let us recall again that Ir^{4+} ions were proven to be generated during the X-ray irradiation of Fe-doped β-Ga_2O_3, as demonstrated by Lenyk et al. [25].

The IR stimulation preceding a TL run (a red line labeled "with IR") reduces the intensities of all the glow peaks, including the 35 and 115 K peaks. This proves that IR stimulation can empty not only Fe^{2+} electron traps but also shallow donor electron traps. We note that for sample A with its relatively low inadvertent Fe content, only a few Fe^{2+} ions and the corresponding low concentrations of the remaining STHs and Fe^{4+} ions would be left after the shallow donor and Fe^{2+} ion traps had been emptied during the IR stimulation. This would differ for thermal stimulation at 35 K during the TL run. Since electrons trapped at Fe^{2+} are not released thermally at low temperatures, more STHs will be saved to produce a somewhat more prominent 115 K glow peak, as observed in the experiment. The same is true of the 205 K peak.

The situation is more complicated for sample B (Fig. 6b, β-Ga_2O_3: Al). Firstly, this sample is insulating at ambient temperatures; therefore, the free carrier concentration is significantly lower than in sample A, and the Fermi level must be lower too. Then, the concentration of inadvertent Fe ions is likely to be higher to achieve full compensation of all the UID background donors with no or less help from uncontrolled Mg contamination, higher in sample A. Since the ltTL spectrum shows a 300 K glow peak, Ir ions must also be considered since the emission ascribed to this peak is supposed to involve Ir ions [18]. We may assume that before the X-ray irradiation, in the dark and at equilibrium, many of the Fe ions will be in the 2+ charge state, and all of the Ir ions will be in the 3+ charge state (the Fermi level pinned at the $Fe^{3+/2+}$ level above the $Ir^{3+/4+}$ level). Since there is no 35 K glow peak, all of electrons generated and trapped at empty, shallow donor levels during the X-ray irradiation preceding the TL run will eventually reside at Fe^{2+} ions, which requires an efficient donor-acceptor charge transfer mechanism and a high enough concentration of Fe^{3+} ions to accept all these electrons. The corresponding valence band holes will be self-trapping as STHs; nevertheless, it has been demonstrated by Lenyk et al. in their study of Ir^{4+} ions in β-Ga_2O_3 [25], that in the absence of a relatively shallow acceptor (such as Mg) and in Fe-doped β-Ga_2O_3, some fraction of the valence band holes may also be captured by the Fe^{3+} and Ir^{3+} ions (converting them to the 4+ charge state). This

explains a dominant 115 K and much smaller 205 (Fe^{3+} hole trap and Fe^{2+} recombination center) and 300 K (Fe^{2+} electron trap and Ir^{4+} recombination center) peak intensities in sample B's blue "no IR" TL glow curve.

It is challenging to develop a detailed scenario explaining the observed changes of the measured red line "with IR" TL glow curve in sample B with the additional IR stimulation (a substantial reduction of the 105 K and an increase of the 300 K peaks). To start, let's suppose that the IR stimulation involves only a transfer of electrons from Fe^{2+} ions to the conduction band (remember that all electrons from the shallow donor traps have already been transferred to Fe^{2+} ions); one would then expect a substantial reduction of the intensity of the 105 K (as observed) and minor but similar changes in the intensities of the remaining glow peaks as concentrations of the holes stored at Fe^{4+} and Ir^{4+} ions would remain unchanged (contrary to the experiment). Some redistribution of holes initiated by the IR light is needed to explain the substantial reduction of the 115 K and a significant enhancement of the 300 K glow peaks after the IR stimulation. So, in addition to the IR-induced transfer of electrons from Fe^{2+} ions to the conduction band, there should also be an IR-driven process of de-trapping of holes from the self-trapped (ST) state that would enable redistribution of holes released by the IR-stimulation to the valence band effectively transferring them from the STH state to Ir^{3+} ($Ir^{3+} \rightarrow Ir^{4+}$) and maybe also Fe^{3+} ($Fe^{3+} \rightarrow Fe^{4+}$) ions. We point out that a similar, although thermally, not optically driven, hole redistribution process between Mg-acceptors and Fe^{3+} ions was reported by Gustafson et al. [15] (see their Fig. 2). Since Mg-acceptors in this sample (below LOQ) are not likely to play any role, it seems possible that the redistribution process will favor Ir not Fe, and most of the holes released from the STH state, which survived recombination generating UV and UV' emission, will be captured by Ir^{3+} ions. Also, the backtransfer of holes to the STH state would be blocked by the IR stimulating laser light increasing the net effect of the IR-irradiation. The 300 K peak in the "with IR" glow curve after the IR stimulation should then gain intensity compared to the 205 K peak, while the 105 K peak would lose, as observed in the experiment.

Both ltTL glow curves of sample C (Fig. 6c, β-Ga_2O_3: Ce), "no IR" and "with IR" alike, are dominated by the 300 K glow peak. Consequently, all electrons and holes that survived recombination generating UV and UV' emissions during the X-ray irradiation preceding a TL run, are stored in this sample at the Fe^{2+} and Ir^{4+} ions so that the emission between 500 and 600 nm, first reported by Lenyk et al. [18], probably dominates the thermoluminescence spectrum also in our experiment.

Sample C is insulating, so in the dark and at equilibrium, all free and donor-bound electrons must be transferred to the compensating Fe^{3+} ions, and the Fermi level will be pinned to the $Fe^{3+/2+}$ acceptor level. There will be no holes or STHs, and all Ir will be in the 3+ charge state. At quasi-equilibrium, following X-ray irradiation at low temperatures (10 K), all electrons will populate Fe ions, and an equal number of holes will be distributed among STHs, Fe^{4+}, and Ir^{4+} ions depending on concentrations of Fe and Ir ions. For high enough concentrations of Ir (we know from the ICP-OES analysis that the Ir concentration is the highest for this sample) most of the holes will end up at the energetically favorable Ir (3+/4+ level). During the TL run, there will be no 35 K peak in the glow curve, and the 105 and 205 K peaks will be reduced. All the surviving electrons and holes, stored at Fe^{2+} and Ir^{4+}, respectively, will recombine at 300 K producing the dominant peak in the glow curve of sample C.

Unfortunately, not much can be inferred from the ltTL glow curves measured for sample D (Fig. 6d, β-Ga_2O_3:Mg) as no glow peaks can be identified in the entire range of temperatures from 10 up to 300 K. This is disappointing as one would expect the Fermi level in this sample at equilibrium (before X-ray irradiation) to be close but below the $Ir^{3+/4+}$ level (the Ir donors very likely provide compensation for the Mg acceptors). The inadvertent Fe ions would be mostly in the 3+ charge state. Therefore during X-ray irradiation, Fe and Mg ions would capture electrons and holes and assume the 2+ and 0 ($Mg^{2+} + O^{1-}$) charge states, respectively. These predictions are confirmed by the EPR experiment; the unexcited Mg-doped and Fe-contaminated β-Ga_2O_3 sample shows the Fe^{3+} and Ir^{4+} but no Mg^0 EPR signals [24]. After the X-ray irradiation, the Fe^{3+} and Ir^{4+} signals are reduced, but Mg^0's increases and becomes visible. (EPR cannot detect the compensated Mg^{-1} ($Mg^{2+} + O^{2-}$) acceptor.) Since the thermal decay of the Mg^0 acceptors was reported to occur at about 250 K [17,32], well below the 300 K thermal stability limit for the Fe^{2+} ions, the mode I recombination between holes released from the Mg^0 and Fe^{2+} ions would seem likely to produce a glow peak at about 250 K. Another option, maybe even more likely, would be to have all the holes transferred to the Ir ions and electrons stored at the Fe^{2+} ions and then the glow peak should appear at 300 K as a result of recombination between electrons released from the $Fe^{2+/3+}$ electron trap and the $Ir^{4+/3+}$ recombination center (the 500–600 nm emission, see Ref. [18]). None of these predicted scenarios for this sample receives any support from our ltTL experiment. The report from previous extensive studies by Luchechko et al. on Mg-doped β-Ga_2O_3 show a range of glow peaks and emissions that does not exclude or specifically point to any of the options discussed above [33].

3.3. *Two-beam experiments (X–IR); results and discussion*

In Figs. 7–10, we present the results of the two-beam experiments on four samples from Table 1 at three different temperatures (10, 100, and 300 K), using three different timing sequences, s1, s2, and s4. In these experiments, we measure the instantaneous, spectrally unresolved radioluminescence intensity as a function of time for a sample excited by an X-ray beam and stimulated by an IR beam from the pulsed infrared laser. The three timing sequences of the X-ray excitation and IR stimulation windows, labeled s1, s2, and s4, are shown schematically at the top of each figure, presenting experimental time waveforms. The X-ray beam was turned on once in each experiment, starting 20 s from the beginning of the experiment (at 0 s) for 120 s. The first IR stimulation window was turned on for 60 s starting at 10 (s2) and 60 s (s4) from the beginning (there was no first IR stimulation window in sequence s1). The second IR stimulation window for all three sequences was turned on at 260 s from the beginning of the experiment and lasted for 180 s. The timing windows lengths and delays for X-rays and IR-light were chosen to enable observation of transient effects and a reasonably accurate estimate of the quasi-equilibrium steady-state radioluminescence intensities.

In Fig. 7, we show the results for sample A. The time waveforms shown in Fig. 7a have been recorded under the constant intensity X-ray excitation in the 120 s time window with no IR stimulation (sequence s1). The 10 and 100 K time waveforms show some residual

transients when the X-ray beam is turned on; there are some rise times and some loss of zero time amplitudes, albeit small and hard to estimate. No transients are observed for the 300 K waveform of Fig. 7a and for any of the three waveforms shown in Fig. 7b (sequence s2).

For sample A we offered an explanation of the TL results (see Fig. 6a) suggesting the participation of the shallow donor traps. This would also explain the missing transients in Fig. 7b and c, as the IR light "disables" these shallow traps by preventing them from filling

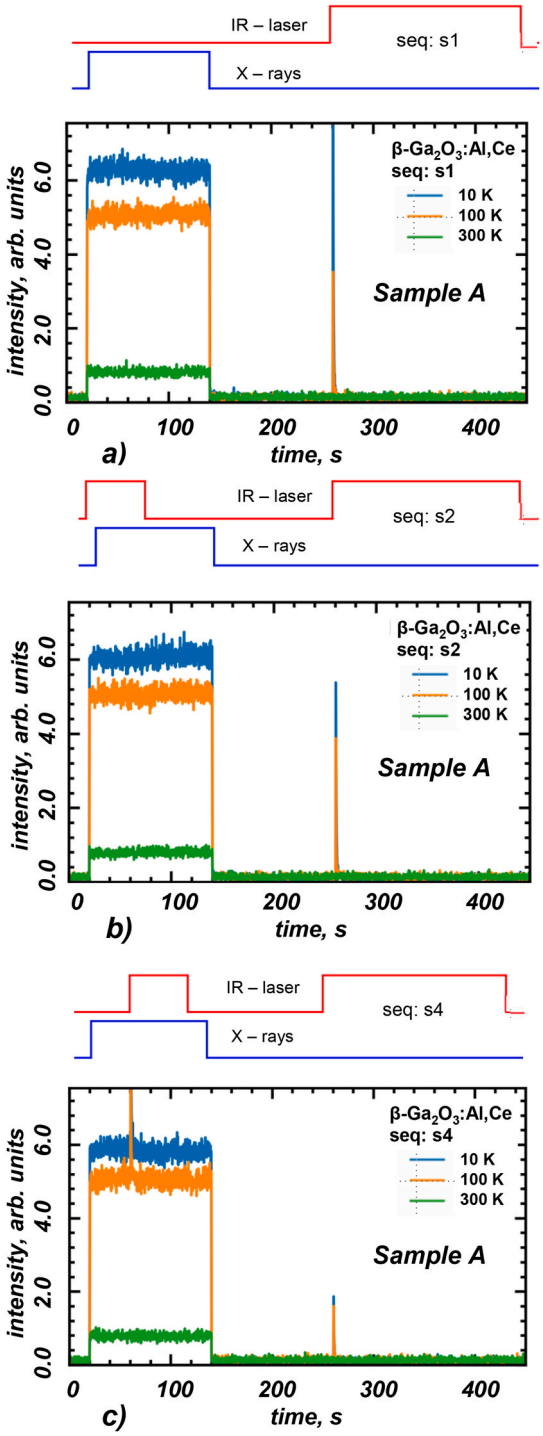

Fig. 7. The wavelength unresolved X–IR two-beam experimental time waveforms for sample A, measured at 10 (blue trace), 100 (orange trace), and 300 K (green trace) for three timing sequences: a) no IR stimulation; sequence s1, b) the IR stimulation window starts 10 s before the X-ray beam is turned on, sequence s2, c) the IR stimulation window starts 40 s after the X-ray beam is turned on, sequence s4.

up, and there simply would be no transient loss of electrons. But then, there also should be no loss of the zero time amplitudes (under IR stimulation). The steady-state intensities with and without IR should not differ and be equal to the value of the zero time transient amplitude (at 10 s, X-rays on) under the IR stimulation.

Consequently, in agreement with and in support of our interpretation of the TL results, we offer the following explanation of the

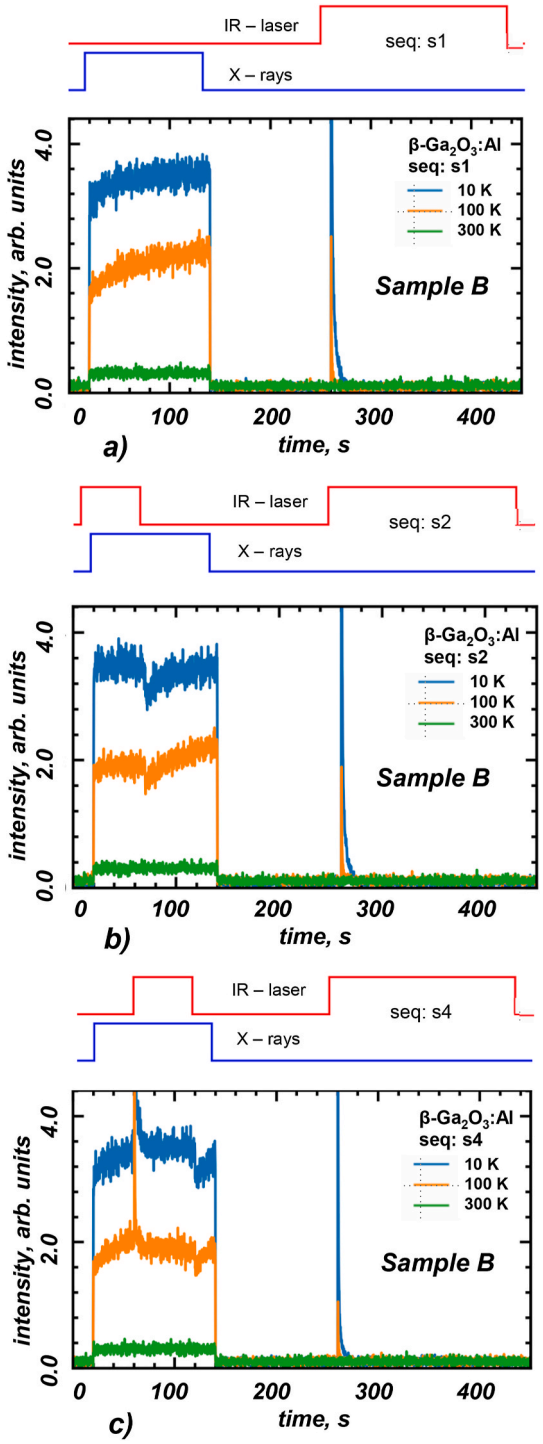

Fig. 8. The wavelength unresolved X–IR two-beam experimental time waveforms for sample B, measured at 10 (blue trace), 100 (orange trace), and 300 K (green trace) for three timing sequences: a) no IR stimulation; sequence s1, b) the IR stimulation window starts 10 s before the X-ray beam is turned on, sequence s2, c) the IR stimulation window starts 40 s after the X-ray beam is turned on, sequence s4.

X–IR results for sample A. In addition to shallow donor traps, we assume that some inadvertent Fe^{3+} ions will behave as electron traps and recombination centers. Also, when the temperature is high enough, an additional recombination path involving Fe^{2+} ions and mobile holes is activated. Before the X-ray irradiation, shallow donor traps, Fe^{3+}, and Fe^{2+} ions were in equilibrium. Then when X-rays are turned on (sequence s1, Fig. 7a, no IR), the conduction band electrons generated by X-rays will be captured by shallow traps and Fe^{3+} ions filling them up ($Fe^{3+} \rightarrow Fe^{2+}$), transient radioluminescence intensities will be reduced, and the waveforms will show rise times.

For sequence s2, Fig. 7b, with the IR light on, the shallow donor and Fe^{3+} electron traps are blocked, most of the shallow donors stay ionized, and there is effectively no conversion $Fe^{3+} \rightarrow Fe^{2+}$. We expect that the zero time amplitudes will increase, and there will be no transients. For the 10 K waveforms, we also expect that the steady state intensities will be lower in the presence of IR stimulation, provided that two conditions are met. Firstly, as expected under IR irradiation, the population of Fe^{3+} ions will increase, and Fe^{2+} ions will decrease. Secondly, the Fe^{3+} ions can capture the valence band holes (as shown to be the case in Ref. [15]) and act as nonradiative recombination centers, while the Fe^{2+} ions can not. At 10 K, the Fe^{2+} ions and STHs are thermally stable and separated, and there should be no (Fe^{2+}, STH) recombination. Consequently, we expect more nonradiative recombination under IR irradiation, and the steady-state UV emission intensities should be lower, as observed. The effect is much weaker for the 100 K waveform (see Fig. 7b) since, at higher temperatures, the self-trapped holes are mobile, both modes of recombination via Fe are active, and the IR irradiation does not make that much of a difference.

In Fig. 8, we show time waveforms for three timing sequences in the X–IR experiment for sample B. Two waveforms of sequence s1, at 10 and 100 K (Fig. 8a, no IR stimulation), in comparison to sample A, show more significant transients; the longer rise times and more prominent differences between the zero-time amplitudes and the steady-state values, indicating loss of light at the onset of the X-ray excitation of about 14 % and at least 40 %, respectively. It is interesting to note that the effect is more significant at 100 K (unlike for sample A) and absent (no transients at all) at 300 K. For sequence s2 (Fig. 8b), transients of 10 and 100 K waveforms at the X-ray onset (20 s from the beginning of the experiment and with the IR stimulation on) almost disappear except for some residual transient at 100 K. The steady-state intensity reaches the value slightly above the zero-time amplitude, nevertheless clearly below the steady-state value to be achieved with no IR. There is also an apparent transient when the IR stimulation is turned off (at 60 s from the beginning of the experiment for sequence s2 and 120 s for sequence s4). The rise times are too long, so for sequence s4 (Fig. 8c) no steady-state conditions are genuinely reached. Still, it is reasonable to assume that the steady-state intensities for the 10 and 100 K waveforms for sequences s2 and s4, with and without IR stimulation, differ. This difference is more prominent at 100 K and much smaller at 10 K. There are no transients and no changes in steady-state intensities for the 300 K waveforms of any sequence for this sample (B).

To explain the X–IR waveforms for sample B, we recall the hole redistribution process proposed for this sample to interpret the ltTL glow curves with and without IR stimulation. We note that the lower Fermi level and the lower free electron concentration in the dark (before X-ray irradiation), in addition to and because of the higher concentration of inadvertent Fe ions, will reduce the concentration and lifetimes of the conduction band electrons under X-ray irradiation. Therefore at 100 K, the thermally activated mobile STHs will now be less likely to recombine with the conduction band electrons and more likely to diffuse and be captured by Ir^{3+} ions so that it will take a longer time to reach equilibrium after the X-rays are turned on, and the fraction of Ir^{3+} ions transformed into the 4+ charge state will increase. This explains the longer rise time and the lower zero-time relative (normalized) amplitude of the 100 K waveform compared to the 10 K waveform. This mechanism will also be responsible for the infra-red stimulated redistribution of holes between STHs and Ir^{3+} during the TL run, as we proposed earlier to explain the TL glow curves of this sample. For sample A this mechanism is less effective because the free electron concentration is higher, and the radiative recombination rates of free electrons and STHs are higher too. The equilibrium will be reached with a lower $Ir^{3+} \rightarrow Ir^{4+}$ conversion ratio and a lower hole contribution to the waveform transient when the X-rays are turned on.

The steady-state intensities are determined by quasi-equilibrium or saturation concentrations of Fe^{2+}, Fe^{3+}, Ir^{3+}, and Ir^{4+}. They are challenging to predict ad hoc and probably hard to obtain reliably by numerical modeling. Also note that some rates, like, e.g. a hole capture rate by Ir^{3+}, although the process is energetically favorable (the $Ir^{3+/4+}$ level is positioned 2.6 eV above the valence band) [21,23,24], may be slow since significant energy differences between levels of ions strongly coupled to the host, and band edges of the host material, usually lead to higher energy barriers and slower rates. This is consistent with the photo-EPR [25] and this experiment (X–IR). Note that below 300 K, the Ir^{3+} ions are likely to work solely as hole traps since both Fe^{2+} and Ir^{4+} ions are, at these temperatures, thermally stable. Low concentrations of the conduction band electrons will reduce both no-UV recombination channels involving the electrons released from the Fe^{2+} and Ir^{4+} ions, and between the conduction band electrons and the Ir^{4+} ions. This explains the origin of transients showing slow increases of the UV contribution to the waveforms when increasing populations of Fe^{4+} and Ir^{4+} ions limit the hole capture rates by Fe^{3+} and Ir^{3+} ions and, therefore, the competition posed by these processes to hole self-trapping, which limits the UV generating recombination between STHs and the conduction band electrons.

We stop here and do not engage in speculations aimed at, e.g., explaining the relations between steady-state intensities and zero-time amplitudes. To reach quasi-equilibrium under constant X-ray excitation, the system must adjust the concentrations of the conduction band electrons, STHs, Fe^{2+}, Fe^{3+}, Ir^{3+}, and Ir^{4+} ions, dependent on the rates of trapping and recombination processes which, in turn, depend not only on the temperature but also on these concentrations. This is not a trivial task since several parameters, such as concentrations, capture cross sections, rates, etc., are involved making numerical modeling of the system difficult and unreliable.

In Fig. 9 we present the results of the X–IR experiment for sample C. From the TL glow curve for this sample we infer that the concentration of inadvertent Fe ions is the highest among the three samples we have considered so far. The dominant glow curve peak is due to the $Fe^{3+/2+}$ electron trap with only a trace indication of the hole self-trap and even less of the $Fe^{3+/4+}$ hole trap peaks.

This would suggest that the electron trapping by the Fe ions (3+ → 2+) mostly balances the hole trapping at Ir (3+ → 4+). Therefore, the hole redistribution process for this sample must be the most efficient one among the three samples considered so far. The

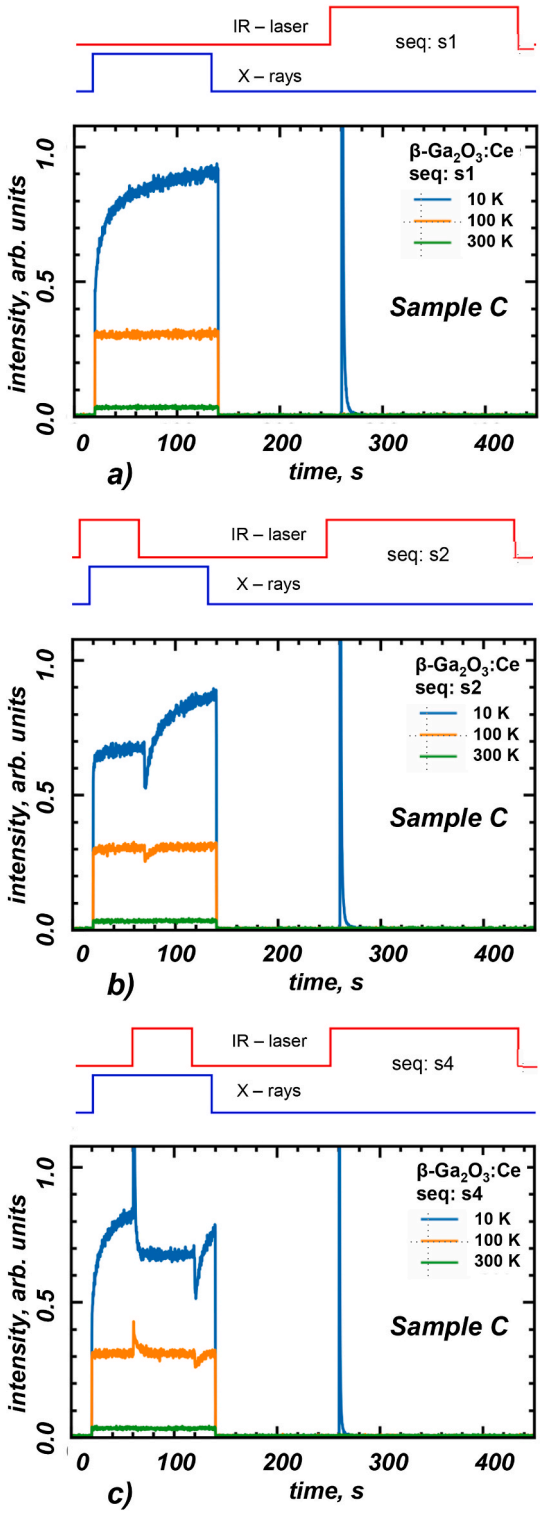

Fig. 9. The wavelength unresolved X–IR two-beam experimental time waveforms for sample C, measured at 10 (blue trace), 100 (orange trace), and 300 K (green trace) for three timing sequences: a) no IR stimulation; sequence s1, b) the 60 s IR stimulation window starts 10 s before the X-ray beam is turned on, sequence s2, c) the 60 s IR stimulation window starts 40 s after the X-ray beam is turned on, sequence s4.

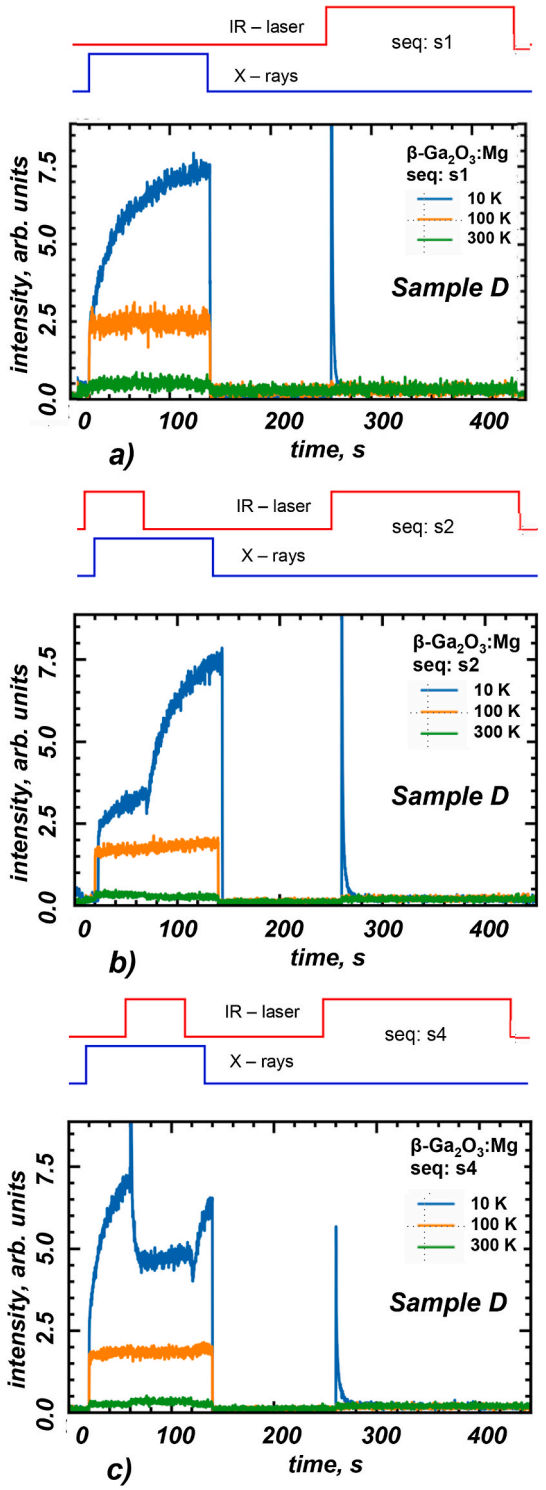

Fig. 10. The wavelength unresolved X–IR two-beam experimental time waveforms for sample D, measured at 10 (blue trace), 100 (orange trace), and 300 K (green trace) for three timing sequences: a) no IR stimulation; sequence s1, b) the 60 s IR stimulation window starts 10 s before the X-ray beam is turned on, sequence s2, c) the 60 s IR stimulation window starts 40 s after the X-ray beam is turned on, sequence s4.

problem with this interpretation is that the hole trapping at Ir^{3+}, from the results obtained for sample B, appears inefficient at 10 K and slow at 100 K. The alternative explanation would be to have a significant fraction of the Ir ions already in the 4+ charge state in the dark (before the X-ray irradiation). This is very unlikely in the sample with no intentional p-type doping, even for intentional and extensive Fe-doping. We do not expect a significant presence of Ir^{4+} in the Fe-doped sample before the X-ray irradiation because the $Fe^{2+/3+}$ acceptor level lies above, and the $Fe^{3+/4+}$ donor level lies below the $Ir^{3+/4+}$ donor level. It is therefore interesting to note that there are reports of the Ir^{4+} presence in the Fe-doped β-Ga_2O_3 in equilibrium (before any irradiation) based on EPR (Lenyk et al. [25]) and IR-absorption (Ritter et al. [34]).

It is, however, irrelevant in our case since the simplest explanation of TL and X–IR results for sample C would require the presence of significant concentrations of Ir^{4+} ions in equilibrium before irradiation. This stands in sharp disagreement with the experiment of Ritter et al. [34] who observe that the Ir^{4+} absorption spectrum is extremely weak and is strongly enhanced by optical excitation with threshold photon energies between 2.2 and 2.3 eV [34]. They suggest that their Fe-doped sample may contain some low concentration acceptor complexes introducing acceptor levels below the $Ir^{3+/4+}$ donor level [34]. We note that in agreement with the conclusions of Ritter et al. [34], Lenyk et al. [25] had to increase the sensitivity of their EPR-spectrometer to record the Ir^{4+} EPR signal from the Fe-doped β-Ga_2O_3 before X-irradiation.

The analysis of the sample C X–IR waveforms shown in Fig. 9 lends, nevertheless, some support for the occurrence of the (Fe^{2+}, Ir^{4+}) recombination channel deduced from the ltTL experiment for this sample. However, unlike in sample B, there is no indication of the thermally activated redistribution process, which is not surprising as there is nothing to redistribute (no 105 K glow peak). The relatively high efficiency of hole-trapping by Ir^{3+} might be due to the unusually high Ir concentration in this particular sample as shown by a direct ICP-OES analysis.

It is interesting to note that the 10 K waveform in Fig. 9b (sequence s2) indicates the presence of two transient components; a relatively fast one prone to the quench by the IR stimulation, dominating the process outside of the IR window, and a slower one, which is not. This slower component shows a small amplitude transient at the onset of X-ray excitation and then slopes up slowly, reaching saturation, as confirmed by the flat part of the 10 K waveform inside the time-shifted IR window, shown in Fig. 9c. The first would be due to electrons captured from the conduction band by Fe^{3+} ions (less trapping, less nonradiative contribution from the remaining Fe^{3+} ions as more Fe ions are now in the recombination-inactive 2+ charge state). The second, slower and IR-independent contribution would be due to the competition for free holes between self-trapping and capture by Ir^{3+} ions that became visible after the Fe-trapping effect had been reduced by IR-irradiation (compare zero-time amplitudes of transients at the onset of X-ray irradiation of 10 K waveforms shown in Fig. 9a–c).

Again, from the lack of slope inside the IR window in the 100 K waveform in Fig. 9c, we infer that the Ir contribution to trapping and loss saturates after about 60 s at some unknown steady-state value, presumably much lower than the zero-time amplitude, which we estimate at 6 % of the maximum steady-state intensity. The loss of the total zero-time amplitude due to the electron and hole trapping and nonradiative recombination involving Fe and Ir at 10 K, referred to the 100 K steady-state intensity taken as a baseline, can be estimated at 65 %, roughly a third of which is due to the nonradiative recombination via Fe^{3+} and Ir^{3+} ions (from the 10 K waveforms of Fig. 9a–b). As already mentioned, the contribution of Ir is most significant at the onset of the X-ray window at about 6 %. The steady-state UV intensity loss due to the recombination via Fe^{3+} can be estimated at 22 % (from the 10 K waveforms of Fig. 9b–c).

Note that the total loss of steady state radioluminescence intensity due to the nonradiative recombination via Fe including both modes of recombination (mode I and II) at 100 K would roughly be about three times higher coming to about 65 % of the 10 K maximum, steady-state radioluminescence intensity.

All those losses are estimated relative to the saturation value of the steady-state UV radioluminescence intensity at 10 K, which is the highest achievable steady-state intensity for the hypothetical sample containing no Fe (all available Fe^{3+} is converted to the 2+ charge state, hence no trapping, and no nonradiative recombination via Fe). Since we did not perform X–IR experiments with a different laser fitting the Ir impurity we are missing data needed to renormalize these estimates by including properly charge trapping and recombination at Ir. All estimates of the zero-time amplitude losses and steady-state UV radioluminescence intensity losses are approximate, sample dependent and, therefore, should be treated with caution.

In Fig. 10, we present the results of the X–IR experiment for sample D. We expect that the Fermi level for this sample will be the lowest among all four samples because of the intentional p-type Mg doping. Since the Mg acceptor level at 0.65 eV above VBM, lies below the $Ir^{3+/4+}$ donor level (2.25–2.30 eV below the CBM) and even below the $Fe^{3+/4+}$ deep donor level at 0.7 eV above the VBM) the Mg ions will be compensated (Mg_{Ga}^{1-} or $Mg^{2+} + O^{2-}$; no hole trapped at any of the O^{2-} ions adjacent to the Mg^{2+} ion) in the unexcited sample at equilibrium, primarily by electrons coming from the shallow donors and Ir^{3+} ions (which then become the ionized shallow donors and Ir^{4+} ions, respectively) [16]. The EPR experiments following the X-ray irradiation reveal the overlapping but resolved spectra of STHs and Mg_{Ga}^{0} ions (no spectrum of Mg_{Ga}^{1+}; two holes) [9,16], so there is, during irradiation, competition for free holes between self-trapping of holes (creation of STHs, $O^{2-} + h_{vb} \rightarrow O^{1-}$) and Mg trapping ($Mg^{2+} + O^{2-} + h_{vb} \rightarrow Mg^{2+} + O^{1-}$). This competition may be far more critical in sample D than the competition between self-trapping and trapping of holes at Ir^{3+} (less Ir^{3+}, more Ir^{4+}), contrary to what we observe in sample C (which contains no Mg). Note also that Ir^{4+} ions may contribute in this sample to extraction of electrons from the conduction band. This prediction is confirmed by the EPR experiments of Lenyk et al. [25].

Interesting and seemingly contradictory statements about the trapping of holes at Mg in two different experiments may also have a bearing on our experiment. Lenyk et al. [25] demonstrate that X-ray irradiation of Mg-doped β-Ga_2O_3 at 77 K easily generates a concentration of Mg_{Ga}^{0} ions producing a relatively large EPR signal measured at 40 K. Interestingly, Lenyk et al. [16] use 325 nm laser light irradiation of the same sample at 120 K to produce the Mg_{Ga}^{0}-EPR signal measured at 50 K clearly of lower relative intensity; moreover, they report to be unable to produce a measurable signal for laser irradiations at temperatures below 90 K but could easily do so when the crystal was held at temperatures above 90 K. Similarly, the crystal irradiated at low temperatures (no signal) and then

warmed to nearly 90 K in the dark would also show a measurable Mg^{0}_{Ga} EPR signal.

The extreme but simplest conjecture would involve valence band holes moving consistently with a band transport mechanism over some limited distance (as opposed to a charge hopping mechanism with no distance limit). It seems hardly unusual since valence band holes self-trap quickly but not immediately; both a self-trapped hole and an Mg-trapped hole involve holes localized at oxygen ions (the threefold coordinated oxygen ion at O(I) position [9,32]). Under higher-density X-ray excitation (to overcome a distance limit for a given Mg concentration), a more significant perturbation of translational symmetry may promote trapping at Mg even at lower temperatures, as observed in the experiment [16,25].

The waveforms shown in Fig. 10 for sample D are similar to those for sample C (Fig. 9), although the transient effects are much more substantial. For no-IR stimulation (sequence s1), the 10 K waveform shows a transient indicating a considerable loss of the zero-time amplitude, the largest among the four samples in this study. The genuine equilibrium is not attained even after 120 s, so the loss must be at least 70 % from Fig. 10a, close to the loss in the steady-state intensity at 10 K, referred to 100 K (at about 77 % from Fig. 10b (s2). The 100 K waveform in Fig. 10a (s1), shows only a weak transient indicating some loss of the zero-time amplitude, and the equilibrium is reached after 20–30 s. The intensity at 300 K is so low that it is nearly impossible to draw meaningful conclusions about transients and steady-state values.

More substantial effects are also observed for the 10 K waveform in Fig. 10b (s2). There are again two transients; one prone to quench by IR-stimulation ($Fe^{3+/2+}$ electron trap) and the second, IR-stimulation independent, which is relatively much more prominent than for sample C. Let us note immediately that this seemingly "IR-stimulation independent" component is not really IR-independent, contrary to sample C. The two adjacent parts inside the IR windows of the 10 K waveforms for sample C (s2 and s4), shown in Fig. 9b–c join smoothly, suggesting that the underlying process (the hole capture by Ir^{3+} ions) is IR-independent, as assumed. This is not the case for sample D; the two parts do not match, and there is no saturation.

A minor contribution to the zero-time amplitude loss would come from the hole trapping at Ir^{3+}, which we proposed as a dominant process for sample C. Since a significant part of Ir ions would now be in the 4+ charge state (Mg compensation), hole trapping by Ir would be reduced, but electron extraction from the conduction band would become more critical. In addition, hole trapping by Mg^{1-}_{Ga} ions certainly contributes significantly to the loss of the zero-time amplitude. Both the electron extraction by Ir and hole-trapping by Mg are likely to dominate the loss of the zero-time amplitude at 10 K for sample D under IR-irradiation (the 10 K waveform, sequence 2, Fig. 10b). Note also that the position of the Ir (3+/4+) level at 2.25–2.30 eV below the CBM makes it insensitive to the IR light. This may not be the case for Mg by analogy; recall that to explain the IR-induced modification of the ltTL glow curve for sample B, we had to assume redistribution of holes released from the self-trapped state by IR stimulation.

Consequently, we propose that the transient in the 10 K waveform of the sequence s1 (Fig. 10a, no IR) has most likely three major components, as suggested by examination of the waveforms shown in Fig. 10b–c and discussion above. The first IR-sensitive component is due to the trap-filling process involving conduction band electrons and Fe^{3+} ions. IR-irradiation transfers all the electrons from the shallow donors and Fe^{2+} ions to the conduction band, just as for the samples discussed previously. The second component would be due to the trap filling process again, but this time involving holes filling the ionized Mg^{1-}_{Ga} acceptors. This process is IR-sensitive as IR stimulation transfers some fraction of STHs and some holes trapped at the Mg^{0}_{Ga} acceptors to the valence band. Electrons and holes released by the IR-laser light to the conduction and valence bands are then trapped/self-trapped and/or recombine, producing positive UV light spikes at the IR-window's onset. Redistribution of holes between Mg ions and STHs under IR stimulation would be responsible for discontinuity in the IR-dependent component in two adjacent IR-windows for 10 K waveforms in Fig. 10b (s2) and 10c (s4).

Assuming that Fe ions are exclusively responsible for the "IR-window" effect in Fig. 10c, we can estimate the steady-state loss of UV intensity due to the recombination via Fe^{3+} at 10 K at about 50 % of the total loss due to the recombination involving both modes of recombination (mode I and II) at 100 K. The IR-insensitive recombination via Ir has not been considered here. More significant losses in zero-time amplitudes are due to trapping at Mg, which is not associated with non-radiative recombination and, therefore, does not contribute to the loss of the steady-state UV intensity. On the contrary, although we are able to make a rough estimate of the contribution to a zero-time amplitude due to the Ir trapping of holes, we are unable to quantify the contribution of the nonradiative recombination via Ir to the loss of the steady-state UV intensity, although there are reasons to suspect it exists (see Gustafson et al. [15] for circumstantial evidence from the thermoluminescence experiment).

4. Summary and conclusions

This paper presents the steady-state radioluminescence spectra for temperatures between 10 and 350 K, low-temperature thermoluminescence glow curves, and two-beam X–IR waveforms measured on four samples of β-Ga_2O_3 single crystals. The crystals were unintentionally doped (UID) with some inadvertent shallow donors (most likely residual Si) and with Fe and Ir unintended impurities leached from the crucibles used to grow these crystals by the Czochralski method. The concentrations of these two impurities were below the reliable detection limit, except for one sample with a higher-than-usual Ir concentration. One sample was intentionally doped with Mg, and one was unintentionally contaminated with Mg at a much lower level. The preceding basic experiments had also been performed on these samples to obtain essential electric and scintillation characterization at ambient temperatures, and the results are collected in Table 1.

We have measured and analyzed the steady-state radioluminescence spectra, thermoluminescence glow curves (with and without the prior IR irradiation), and the X–IR double beam waveforms for these samples. The measured glow curves display several glow peaks to which we assign traps and recombination centers following conclusions and suggestions published earlier (see the Introduction for a detailed summary). We find that the varying concentration of inadvertent Fe ions becomes the most critical variable

factor responsible for differences in the glow curves of these samples.

The X–IR waveforms show steady-state radioluminescence intensity changes, and transients in response to the changes in the X-ray excitation and IR stimulation. These changes and IR-induced transients, similar to the thermoluminescence glow curves, also depend on Fe concentration. The experimental results of both experiments and their interpretations in terms of traps and recombination centers are consistent.

From the X–IR waveforms measured at different temperatures, we find that the total loss of steady state wavelength integrated radioluminescence intensity between 10 and 100 K for sample A Fig. 7a, is about 20 %; for sample B Fig. 8a, it is 33 %; for sample C Fig. 9a, it is 66 %; and for sample D Fig. 10a, it is 68 %. This loss becomes even higher at 300 K for all samples, nearly 90 % for sample A, 93 % for sample B, 97 % for sample C, and 98 % for sample D.

By comparing steady-state intensities with and without IR stimulation in the 10 K waveforms, we can estimate the loss incurred when most of the Fe ions are in the 3+ charge state. Reliable estimates for samples A and B are difficult to obtain; for sample C, this loss is 18 %, and for sample D is 32 %. The loss due to the Fe^{2+} is insignificant at 10 K. Still, it increases with the temperature, saturating at about 100–120 K. For higher temperatures up to 300 K, the combined loss involving both recombination routes of Fe is snowballing rapidly due to the increased possibility of multiple de-trapping of the STHs.

We speculate that the concentration of Ir^{4+} ions in the heavy Ir-contaminated samples may proliferate via the redistribution of holes at higher temperatures, increasing the loss of UV radioluminescence. The effect would likely be more substantial in samples containing more significant concentrations of Fe and, particularly, Mg. Quantitative estimates, unfortunately, are highly speculative and unreliable.

In conclusion, semi-insulating (Fe and Mg-doped) β-Ga_2O_3 single crystals are not recommended as scintillators in β-Ga_2O_3 based devices. Ir in crystals free of Fe and Mg may be tolerable.

Data availability statement

Data will be made available on request.

CRediT authorship contribution statement

A.J. Wojtowicz: Writing – review & editing, Writing – original draft, Methodology, Investigation, Formal analysis, Conceptualization. **M.E. Witkowski:** Visualization, Software, Investigation, Formal analysis, Data curation. **W. Drozdowski:** Writing – review & editing, Project administration, Methodology, Investigation, Funding acquisition, Data curation, Conceptualization. **M. Makowski:** Software, Investigation. **Z. Galazka:** Writing – review & editing, Project administration, Investigation, Funding acquisition, Formal analysis.

Declaration of competing interest

The authors declare that they have no known competing financial interests or personal relationships that could have appeared to influence the work reported in this paper.

Acknowledgements

The authors would like to thank Dr. Andrea Dittmar (Leibniz-Institut für Kristallzüchtung) for measurements of impurities in investigated samples by ICP-OES. This research has been financed from the funds of the Polish National Science Centre (NCN) and the German Research Foundation (DFG) in frames of a joint grant (NCN: 2016/23/G/ST5/04048, DFG: GA 2057/2–1).

References

[1] Z. Galazka, Growth of bulk β-Ga_2O_3 single crystals by the Czochralski method, Appl. Phys. 131 (2022), 031103.
[2] T. Yanagida, G. Okada, T. Kato, D. Nakauchi, S. Yanagida, Fast and high light yield scintillation in the Ga_2O_3 semiconductor material, Appl. Phys. Express 9 (2016), 042601.
[3] W. Drozdowski, M. Makowski, M.E. Witkowski, A.J. Wojtowicz, Z. Galazka, K. Irmscher, R. Schewski, β-Ga_2O_3:Ce as a fast scintillator: an unclear role of cerium, Radiat. Meas. 121 (2019) 49–53.
[4] Marek Moszynski, Agnieszka Syntfeld-Każuch,Kamil Brylew, Private Communication..
[5] W. Drozdowski, M. Makowski, A. Bachiri, M.E. Witkowski, A.J. Wojtowicz, L. Swiderski, K. Irmscher, R. Schewski, Z. Galazka, Heading for brighter and faster β-Ga_2O_3 scintillator crystals, Opt. Mater. X 15 (2022), 100157.
[6] V.B. Mykhaylyk, H. Kraus, V. Kapustianyk, M. Rudko, Low temperature scintillation properties of Ga_2O_3, Appl. Phys. Lett. 115 (2019), 081103.
[7] W.C. Herbert, H.B. Minier, J. Brown, Jr, Self-activated luminescence of β-Ga_2O_3, J. Electrochem. Soc. 116 (1969) 1019.
[8] T. Harwig, F. Kellendonk, S. Slappendel, The ultraviolet luminescence of β-gallium sesquioxide, J. Phys. Chem. Solid. 39 (1978) 675–680.
[9] B.E. Kananen, N.C. Giles, L.E. Halliburton, G.K. Foundos, K.B. Chang, K.T. Stevens, Self-trapped holes in β-Ga_2O_3 crystals, J. Appl. Phys. 122 (2017), 215703.
[10] J.B. Varley, A. Janotti, C. Franchini, C.G. Van de Walle, Role of self-trapping in luminescence and p-type conductivity of wide-band-gap oxides, Phys. Rev. B85 (R) (2012), 081109.
[11] K. Irmscher, Z. Galazka, M. Pietsch, R. Uecker, R. Fornari, Electrical properties of β-Ga_2O_3 single crystals grown by the Czochralski method, J. Appl. Phys. 110 (2011), 063720.
[12] B.E. Kananen, L.E. Halliburton, K.T. Stevens, G.K. Foundos, N.C. Giles, Gallium vacancies in β-Ga_2O_3 crystals, Appl. Phys. Lett. 110 (2017), 202104.
[13] T. Harwig, F. Kellendonk, Some observations on the photoluminescence of doped β-gallium sesquioxide, J. St. Chem. 24 (1978) 255–263.

[14] M.E. Ingebrigtsen, J.B. Varley, A.Yu Kuznetsov, B.G. Svensson, G. Alfieri, A. Mihaila, U. Badstubner, L. Vines, Iron and intrinsic deep level states in Ga_2O_3, Appl. Phys. Lett. 112 (2018), 042104.
[15] T.D. Gustafson, C.A. Lenyk, L.E. Haliburton, N.C. Giles, Deep donor behavior of iron in β-Ga_2O_3 crystals: establishing the $Fe^{4+/3+}$ level, J. Appl. Phys. 128 (2020), 145704.
[16] C.A. Lenyk, T.D. Gustafson, S.A. Basun, L.E. Haliburton, N.C. Giles, Experimental determination of the (0/-) level for Mg acceptors in β-Ga_2O_3 crystals, Appl. Phys. Lett. 116 (2020), 142101.
[17] N.B. Polyakov, I.V. Smirnov, S.J. Shchemerov, Fan Ren Pearton, A.V. Chernykh, A.J. Kochkova, Electrical properties of bulk semi-insulating β-Ga_2O_3 (Fe), Appl. Phys. Lett. 113 (2018), 142102.
[18] C.A. Lenyk, T.D. Gustafson, L.E. Haliburton, N.C. Giles, Deep donors and acceptors in β-Ga_2O_3: determination of the $Fe^{3+/2+}$ level by a noncontact method, J. Appl. Phys. 126 (2019), 245701.
[19] M. Kleverman, P. Omling, L.-Å. Ledebo, H.G. Grimmeiss, Electrical properties of Fe in GaAs, J. Appl. Phys. 54 (1983) 814.
[20] E. Malguth, A. Hoffmann, W. Gehlhoff, O. Gelhausen, M.R. Phillips, X. Xu, Structural and electronic properties of Fe^{3+} and Fe^{2+} centers in GaN from optical and EPR experiments, Phys. Rev.. B74 (2006), 165202.
[21] J.R. Ritter, J. Huso, P.T. Dickens, J.B. Varley, K.G. Lynn, M.D. McCluskey, Compensation and hydrogen passivation of magnesium acceptors in β-Ga_2O_3, Appl. Phys. Lett. 113 (2018), 052021.
[22] P. Seyidov, M. Reimsteiner, Z. Galazka, K. Irmscher, Resonant electronic Raman scattering from Ir^{4+} ions in β-Ga_2O_3, J. Appl. Phys. 131 (2022), 035707.
[23] S. Bhandari, M.E. Zvanut, Charge trapping at Fe due to midgap levels in β-Ga_2O_3, J. Appl. Phys. 129 (2021), 085703.
[24] S. Bhandari, M.E. Zvanut, J.B. Varley, Optical absorption of Fe in doped Ga_2O_3, J. Appl. Phys. 126 (2019), 165703.
[25] C.A. Lenyk, N.C. Giles, E.M. Scherrer, B.E. Kananen, L.E. Hallburton, K.T. Stevens, G.K. Foundos, J.D. Blevins, D.L. Dorsey, S. Mou, Ir^{4+} ions in β-Ga_2O_3 crystals: an unintentional deep donor, J. Appl. Phys. 125 (2019), 045703.
[26] N.R.J. Poolton, B.M. Towlson, D.A. Evans, B. Hamilton, Synchrotron–laser interactions in hexagonal boron nitride: an examination of charge trapping dynamics at the boron K-edge, New J. Phys. 8 (2006) 76.
[27] M.D. McCluskey, Point defects in Ga_2O_3, J. Appl. Phys. 127 (2020), 101101.
[28] Z. Galazka, S. Ganschow, A. Fiedler, R. Bertram, D. Klimm, K. Irmscher, R. Schewski, M. Pietsch, M. Albrecht, M. Bickermann, Doping of Czochralski-grown bulk β-Ga_2O_3 single crystals with Cr, Ce and Al, J. Cryst. Growth 486 (2018) 82–90.
[29] M.E. Witkowski, K.J. Drozdowski, M. Makowski, W. Drozdowski, A.J. Wojtowicz, K. Irmscher, R. Schewski, Z. Galazka, Low temperature thermoluminescence of β-Ga_2O_3 scintillator, Opt. Mater. X 16 (2022), 100210.
[30] R. Heitz, P. Maxim, L. Eckey, P. Thurian, A. Hoffmann, I. Broser, K. Pressel, B.K. Meyer, Excited states of Fe^{3+} in GaN, Phys. Rev. B 55 (1997) 4382.
[31] R. Sun, Y.K. Ooi, P.T. Dickens, K.G. Lynn, M.A. Scarpulla, On the origin of red luminescence from iron-doped β-Ga_2O_3 bulk crystals, Appl. Phys. Lett. 117 (2020), 052101.
[32] B.E. Kananen, L.E. Halliburton, E.M. Scherrer, K.T. Stevens, G.K. Foundos, K.B. Chang, N.C. Giles, Electron paramagnetic resonance study of neutral Mg acceptors in β-Ga_2O_3 crystals, Appl. Phys. Lett. 111 (2017), 072102.
[33] A. Luchechko, V. Vasyltsiv, L. Kostyk, O. Tsvetkova, A.I. Popov, Shallow and deep trap levels in X-ray irradiated β-Ga_2O_3:Mg, Nucl. Instrum. Methods Phys. Res. B 441 (2019) 12–17.
[34] J.R. Ritter, L.G. Lynn, M.D. McCluskey, Iridium-related complexes in czochralski-grown β-Ga_2O_3, J. Appl. Phys. 126 (2019), 225705.